Winter observations of CO_2 exchange between sea-ice and the atmosphere in a coastal fjord environment

(Journal: The Cryosphere)

Jakob Sievers[1,3], Lise Lotte Sørensen[1,3], Tim Papakyriakou[5], Brent Else[7], Mikael K. Sejr[2,3], Dorte Haubjerg Søgaard[4,8], David Barber[5], Søren Rysgaard[3,4,5,6]

[1] [Department of Environmental Science, Aarhus University, 4000 Roskilde, Denmark]

[2] [Department of Bioscience, Aarhus University, 8600 Silkeborg, Denmark]

[3] [Arctic Research Centre, Aarhus University, 8000 Aarhus, Denmark]

[4] [Greenland Climate Research Centre, c/o Greenland Institute of Natural Resources box 570, Nuuk, Greenland.]

[5] [Centre for Earth Observation Science, CHR Faculty of Environment Earth and Resources, University of Manitoba, 499 Wallace Building Winnipeg, MB R3T 2N2, Canada.]

[6] [Department of Geological Sciences, University of Manitoba, Winnipeg, Winnipeg, MB R3T 2N2, Canada.]

[7] [Department of Geography, University of Calgary, Calgary, AB T2N 1N4, Canada.]

[8] [Department of Biology, University of Southern Denmark, Campusvej 55, 5230 Odense M, Denmark]

Correspondence to: J. Sievers (jasi@envs.au.dk)

Abstract

Eddy covariance observations of CO_2-fluxes were conducted during March-April 2012 in a temporally sequential order for 8, 4 and 30 days respectively, at three locations on fast sea-ice and on newly formed polynya ice in a coastal fjord environment in North East Greenland. CO_2 fluxes at the sites characterized by fast sea ice (ICEI and DNB) were found to increasingly reflect periods of strong outgassing in accordance with the progression of springtime warming and the occurrence of strong wind events: $\mathrm{F_{CO2}^{ICE1}} = 1.73 \pm 5\ \mathrm{mmol\,m^{-2}d^{-1}}$ and $\mathrm{F_{CO2}^{DNB}} = 8.64 \pm 39.64\ \mathrm{mmol\,m^{-2}d^{-1}}$, while CO_2 fluxes at the polynya site (POLYI) were found to generally reflect uptake $\mathrm{F_{CO2}^{POLY1}} = -9.97 \pm 19.8\ \mathrm{mmol\,m^{-2}d^{-1}}$. Values given are the mean and standard deviation, and negative/positive values indicate uptake/outgassing respectively. A diurnal correlation analysis supports a significant connection between site energetics and CO_2-fluxes linked to a number of possible thermally driven processes, which are thought to change the pCO_2 gradient at the snow-ice interface. The relative influence of these processes on atmospheric exchanges likely depends on the thickness of the ice. Specifically, the study indicates a predominant influence of brine volume expansion/contraction, brine dissolution/concentration and calcium carbonate formation/dissolution at sites characterized by a thick sea ice cover, such that surface warming leads to an uptake of CO_2 and vice versa, while convective overturning within the sea ice brines dominate at sites characterized by comparatively thin sea ice cover, such that nighttime surface cooling leads to an uptake of CO_2 to the extent permitted by simultaneous formation of superimposed ice in the lower snow-column.

1 Introduction

Sea-ice has long been considered a passive participant in the high latitude carbon cycle, preventing CO_2 exchange between the ocean and atmosphere. Consequently, most carbon-cycle research has treated ice-cover as areas of zero (or very low) exchange (Tison et al., 2002). This view has been challenged by reports of significant fluxes of CO_2 over first and multiyear sea-ice during both spring/summer (Delille et al., 2007; Geilfus et al., 2012; Papakyriakou and Miller, 2011; Semiletov et al., 2004; Semiletov et al., 2007; Zemmelink et al., 2006) and autumn/winter (Else et al., 2011; Geilfus et al., 2013; Miller et al., 2011a; Miller et al., 2011b) and suggestions of a coupling between the carbonate system in sea ice, the underlying sea water and the atmosphere (Anderson et al., 2004;

Nomura et al., 2006; Papadimitriou et al., 2004; Rysgaard et al., 2011; Rysgaard et al., 2012; Rysgaard et al., 2007; Rysgaard et al., 2013).

The coupling of the air-ice-ocean carbonate system has been suggested to drive a significant annual net uptake of CO_2, through convective sequestration of CO_2 to intermediate and deeper ocean layers during wintertime sea ice formation and subsequent CO_2 uptake from the atmosphere during springtime sea-ice melt (Rysgaard et al., 2009; Rysgaard et al., 2007). Together with seasonal biological carbon uptake within the ice (Thomas and Dieckmann, 2010; Lizotte, 2001), this outlines the basis for a seasonal carbon imbalance, which may drive CO_2 uptake from the atmosphere during springtime melting of sea-ice, and mineral dissolution of trapped calcium carbonate ($CaCO_3$) within the brine channels. The net uptake associated with this sea ice-driven carbon pump has been estimated to be $50 \mathrm{MT\,C\,yr^{-1}}$ in the Arctic alone (Rysgaard et al., 2007) and constitutes an important fraction of the total CO_2 uptake of the Arctic Ocean $(66 - 199 \mathrm{MT\,C\,yr^{-1}})$ (Parmentier et al., 2013). The size of these estimates highlights the importance of the annual sea ice cycle on the global carbon cycle, particularly since the sea ice cover is becoming more ephemeral over a range of space and time scales (Barber et al., 2014).

Accurate assessment of the impact of air-ice-ocean CO_2 exchanges on the global carbon budget in a future climate requires the continued advancement of exchange parameterizations and up-scaling techniques that describe CO_2 exchange within all sea-ice conditions, as well as particularly dynamic areas such as polynyas, leads, cracks and thaw-holes. To our knowledge only one attempt has been made at developing a parameterization for air - sea ice CO_2 exchanges in a fast ice environment (Sørensen et al., 2014). That study emphasizes the importance of, and difficulties in, estimating the surface pCO_2 concentration in sea ice in order to make a proper parameterization. In general there is a need for further investigations into the interplay between biogeochemical and physical processes in facilitating and mediating observed air - sea ice CO_2 exchanges. Such efforts are, however, complicated by the logistical limitations associated with conducting large-scale observations in the Arctic, and the prerequisite requirement of providing trustworthy data from an inhospitable and instrument-challenging environment. From a surface-flux perspective, recent studies have suggested that some open path infrared gas analyzers, commonly used to conduct eddy covariance observations (e.g. Baldocchi, 2008) of CO_2 fluxes, may be subject to sensor bias during cold weather application (Papakyriakou and Miller, 2011, and references herein). A recent study furthermore found that eddy covariance flux estimates in environments characterized by very small scalar fluxes, such as sea ice, are likely to be influenced by larger scale motions, making it difficult to accurately resolve vertical turbulent fluxes under these conditions (Sievers et al., 2015).

Here we present an investigation into connections between site surface energetics, wind speed and CO_2 fluxes over snow covered sea ice during a 6-week field experiment in late winter (March-April) of 2012 in the fast sea ice and polynya environment of Young Sound, NE Greenland. Measurements were conducted with gas analyzers believed to be less sensitive to temperature biases relative to previous reported studies, while eddy covariance flux estimates were derived using the Ogive optimization method (Sievers et al., 2015) that accounts for the problem of influence from large scale motions in low-flux environments.

2 Theory and Method

2.1 Study location and instrumentation

Observations of CO_2-exchanges were carried out from early March to late April of 2012 in the vicinity of the Daneborg base in Young Sound, NE Greenland (Fig. 1). During the campaign two separate flux towers, one stationary and one mobile, were used at three different locations (ICEI, POLYI and DNB). Data from ICEI and POLYI were used in a recent study concerning the distribution of ikaite crystals ($CaCO_3{\cdot}H_2O$) in sea ice (Rysgaard et al., 2013). Data were collected at ICEI (74°18.576'N, 20°18.275'W) and DNB (74°18.566'N, 20°13.998'W) from the 20th-27th of March and the 29th of March to the 27th of April respectively. Both were located inside Young Sound in conditions of 110-115 cm thick sea ice and 67-88 cm snow cover thickness. Data were collected at POLYI (74°13.883'N, 20°07.758'W) from the 24th -27th of March at the mouth of the sound in an active polynya area. Conditions at the site were distinctly different from those of ICEI and DNB, with 15-30 cm ice thickness and 15-20 cm snow cover thickness (Barber et al., 2014).

Observations of the three wind components and CO_2 at the static site (ICEI) were performed with a Gill Windmaster sonic (Gill Instruments®, Lymington UK) and an LI-7200 closed path gas analyzer (LI-COR®, Licoln, NE, USA), placed 3.8 m and 3.5 m above the snow surface respectively, with a horizontal separation of 0.42 m. Observation frequency was 10 Hz. Any frosting on the sensors was removed during daily maintenance, and datasets were discarded accordingly based on instrument diagnostics output. In addition a number of datasets were discarded due to unfavourable wind directions for which the flow was potentially disturbed by the tower itself. Net radiation was recorded with a Kipp & Zonen CNR1 net radiometer (Kipp & Zonen®, Delft, The Netherlands) placed 1.00 m above the undisturbed snow surface. Observations of the wind components and CO_2 at the mobile site (POLYI and DNB) were performed with a METEK USA-1 sonic anemometer (METEK®, Elmshorn, Germany) and a LI-7500A (LI-COR®, Licoln, NE, USA) gas analyzer, placed 3.1 m and 2.7 m above the snow-surface, with a horizontal separation of 0.44 m. Observation frequency was 20 Hz. As at ICEI, a number of datasets were discarded because of frosting on the sensors and unfavourable wind direction. At the POLYI site net radiation was recorded with a Kipp & Zonen CNR1 net radiometer (Kipp & Zonen®, Delft, The Netherlands). At the DNB site no on-site net radiometer data were available. Over this period we make use of radiation measurements made with a Kipp & Zonen CMA6 and a Kipp & Zonen NR lite net radiometer (Kipp & Zonen®, Delft, The Netherlands) located in Zackenberg research station (74°28.315'N, 20°33.125'W), approximately 20 km further in-sound relative to the Daneborg base (Fig. 1). Air temperature was observed at ICEI and POLYI using Campbell Scientific HMP45C212 sensors (Campbell Scientific®, UT, USA). Chamber observations of CO_2 flux were carried out at sites ICEI and POLYI using an LI-8100A (LI-COR®, Licoln, NE, USA) automated soil CO_2-flux chamber system. Sea ice cores were extracted at all sites using a MARK II coring system (Kovacs Enterprises). Temperature readings were performed on all cores, while the sea ice cores from ICEI and POLYI were subjected to additional brine volume calculation as described in (Rysgaard et al., 2013).

2.2 Flux measurements and analysis

While the LI-7200 gas analyzer (ICEI) utilizes measurements of temperature, pressure, and water vapour within the gas analyzer cell to make point-by-point calculations of dry air mixing ratio, the open path LI-7500A gas analyzer (POLYI and DNB) requires a density correction based on external measurements of temperature and pressure. This was achieved using the point-by-point method described by Sahlee et al. (2008), with fast measurements of temperature and pressure provided by the sonic anemometer. Subsequently, surface flux estimates of CO_2, sensible and latent heat were derived using Ogive optimization (Sievers et al., 2015). The approach allows for separation of vertical turbulent flux and contributions from larger scale motions by optimization of a model Ogive spectral distribution (Desjardins et al., 1989; Foken et al., 2006) to a density distribution of a large number of Ogive spectral distributions, for which dataset length and de-trending by running mean are varied simultaneously. Flux estimates are discarded only if an excessive number of gaps are present in the raw dataset or if no theoretical model Ogive distribution can be optimized sufficiently. Among a number of other desirable attributes, the method does not require the application of any conventional spectral corrections, making flux estimates less likely to reflect propagation of uncertainties associated with serial-correction. In this study we adopt the standard convention that all turbulent fluxes are negative towards the surface and positive away from the surface.

2.3 The surface energy balance

Following e.g. (Else et al., 2014; Persson, 2012) the surface energy balance of snow overlaying sea-ice may be written as:

$$\Delta Q = -R_{net} - Q_{SENS} - Q_{LAT} - G \qquad (1)$$

where ΔQ is the net energy flux at the surface Q_{SENS} is the turbulent sensible heat flux, Q_{LAT} is the turbulent latent heat flux and G is the upward conductive heat through the snow and ice. The net radiative flux may be written as:

$$R_{net} = R_n^{SW} + R_n^{LW} - R^T \qquad (2)$$

where R_n^{SW} and R_n^{LW} are the net shortwave ($0.3\mu m - 5\mu m$) and longwave ($5\mu m - 40\mu m$) radiative fluxes respectively, R^T is the net radiative energy transmitted into the snow cover. The latter is derived here based on Persson (2012, eq. 10). We deviate from Persson (2012) by treating all terms as positive if energy is transported away from the surface and negative otherwise, thus conforming to the conventions of turbulent fluxes, to simplify interpretation of a correlation analysis, which follows in a subsequent section. Using this notation, ΔQ, will be positive when net energy is received by the snow/ice volume, and negative when net energy is lost. While R_n^{LW}, Q_{SENS} and Q_{LAT} are exchanged virtually at the snow surface, R_n^{SW} penetrates into the snow/ice cover where it is strongly attenuated with depth. Following (Persson, 2012, eq. 10) we can derive a 1% transmission rate at 0.46 m depth into snow, suggesting that for very thick snow covers, energy transport to the snow/ice interface relies on other mechanisms. Energy transport within a snow cover occurs mainly as conduction between snow-grains and as vapour transport (Sturm et al., 2002). Upward vapour transport by thermal convection has been shown to occur in terrestrial snow covers (Powers et al., 1985) and to depend on medium porosity and the strength of the temperature gradient within the medium (Ganot et al., 2014; Sturm, 1991).

2.4 Thermochemical carbon processes in the ice

Brine volume decreases with decreasing sea-ice temperature. This can lead to significant changes in the mineral-liquid thermodynamic equilibrium of the brine and to thermally sequential mineral precipitation (Marion, 2001), most notably of calcium carbonate in the form of the metastable mineral *ikaite* $(CaCO_3 \cdot 6H_2O)$ at temperatures below -2.2°C:

$$Ca^{2+} + 2HCO_3^- \leftrightarrow CaCO_3 + H_2O + CO_{2(aq)} \quad (3)$$

The formation of $CaCO_3$ and $CO_{2(aq)}$ and the decreasing CO_2 solubility of the increasingly saline brine (Tison et al., 2002), drives the brine to higher CO_2 partial pressure (pCO_2) (Geilfus et al., 2012). Hence, the temperature sensitivity of carbon speciation in sea ice brines supports the premise that thermochemical processes within brine exposed to the atmosphere facilitates an air-ice pCO_2 gradient, thereby linking CO_2 exchange to site energetics via brine carbon chemistry (Loose et al. 2011). In theory, sea ice is permeable to vertical brine transport when brine proportion by volume in sea ice is in excess of $\sim5\%$ (Golden et al., 1998). The brine-atmosphere interface may be positioned at the sea ice surface or at distance up into the snow pack as would be the case for brine-wetted snow. Snow over sea ice may contain appreciable quantities of salt, drawn up from the ice surface in the form of concentrated brine (Barber et al., 1995a; Barber et al., 1995b; Crocker, 1984; Perovich and Richtermenge, 1994). A list of processes possibly affecting pCO_2 at the brine-atmosphere interface include; (1) Given sufficiently permeable sea-ice (Golden et al., 1998; Loose et al., 2011a; Loose et al., 2011b) brine concentration/dilution, alters the pCO_2 gradient across the sea-ice surface and thus the potential for CO_2 exchanges (Geilfus et al., 2012; Killawee et al., 1998; Tison et al., 2002; Nomura et al., 2006; Papadimitriou et al., 2004). (2) Formation/dissolution of calcium carbonate ($CaCO_3{\cdot}6H_2O$) within brine (Dieckmann et al., 2008; Fischer et al., 2013; Marion, 2001; Papadimitriou et al., 2004; Rysgaard et al., 2013) leads to an increase/decrease in brine pCO_2 thus changing the potential for CO_2 exchanges at the ice surface (Geilfus et al., 2012; Miller et al., 2011b; Papakyriakou and Miller, 2011; Sogaard et al., 2013). (3) $CaCO_3{\cdot}6H_2O$ has been observed in brine-soaked snow at the snow/ice interface (Fischer et al., 2013; Geilfus et al., 2013; Nomura et al., 2013). This suggests that formation/dissolution of $CaCO_3{\cdot}6H_2O$ in snow may be able to contribute to observed CO_2 exchange, particularly during conditions conducive to upward transport of brine to the snow base from the sea ice (e.g. large snow/ice interface brine volume and negative freeboard).

2.5 Gas transport in snow

Gas transport in snow occurs by way of diffusion, advection and thermal convection. While diffusion is a slow process, and thermal convection is a notoriously elusive process (Powers et al., 1985), advection, or wind-pumping, is a dynamic process that allow for very rapid flushing of CO_2, which has been accumulated in the snow-pockets (Jones et al., 1999; Sturm, 1991) following e.g. emission from the sea-ice. The wind pumping process has been described in a number of studies (Albert et al., 2002; Albert and Shultz, 2002; Jones et al., 1999; Massman and Frank, 2006; Seok et al., 2009; Takagi et al., 2005) as well as discussed specifically as a plausible mechanism for periods of enhanced CO_2 exchanges on sea-ice (Miller et al., 2011b; Papakyriakou and Miller, 2011).

3 Observations

3.1 ICEI

Freeboard, which is the height of the ice above the water surface, was found at ICEI to be negative and a thin slush layer was observed at the snow/ice interface. Observed CO_2 fluxes, energy fluxes, and meteorological parameters from the site are shown in Fig. 2. The site experienced a number of power outages, primarily during night and in the morning, as indicated by instrument status bars (Fig. 2A). The prevailing wind direction (Fig. 2A) during the ICEI experiment was from the ice covered inner fjord (North). The period was dominated by low wind speeds on the order of $1 - 2\ \mathrm{ms^{-1}}$ with three events of relatively strong wind-speed $\mathrm{U} = 6 - 8\ \mathrm{ms^{-1}}$ recorded on the evening of the 20th of March, past midday on the 25th of March and during night on the 26th of March respectively (Fig. 2A). Air temperature was recorded within the range $\mathrm{T_{air}} = -25 \pm 10°\mathrm{C}$ and followed a diurnal pattern with daily temperature changes on the order of $10 - 15°\mathrm{C}$ (Fig. 2A). The range of CO_2 fluxes observed at ICEI (Fig. 2A) was modest and characterized by limited variation; $\mathrm{F_{CO2}} = 1.73 \pm 5\ \mathrm{mmol\,m^{-2}d^{-1}}$, where values given are the mean and standard deviation. Two chamber observations were conducted just before midday on the 25th of March (Fig. 2A, magenta diamonds), both showing flux estimates similar to eddy covariance derived flux estimates at the same time during both the preceding and the following day ($\mathrm{F_{CO2}} = 0.86\ \mathrm{mmol\,m^{-2}d^{-1}}$ and $\mathrm{F_{CO2}} = 2.16\ \mathrm{mmol\,m^{-2}d^{-1}}$). No concurrent eddy covariance observations were available. Average net solar radiation during the experiment was low $\mathrm{\overline{R}_n^{SW}} = -27\mathrm{Wm^{-2}}$ (Fig. 2B). Sensible heat fluxes were predominantly within the range $\mathrm{Q_{SENS}} = \pm 5\ \mathrm{Wm^{-2}}$ with three events of strong warming and cooling $\mathrm{Q_{SENS}} = \pm 25\ \mathrm{Wm^{-2}}$ recorded on the evening of the 20th of March, the evening and night of the 25th -26th of March and the night of the 26th-27th of March, respectively (Fig. 2C). The only non-negligible latent heat fluxes were recorded on the night of the 26th-27th of March within the range $\mathrm{Q_{LAT}} = 2 \pm 2\ \mathrm{Wm^{-2}}$ (Fig. 2C). Ice-temperatures taken from an extracted ice-core on the 17th of March, three days before the initiation of the experiment, indicated a snow/ice interface temperature at $-10°\mathrm{C}$ and calculated brine volume at around $\mathrm{V_B} = 5.1\%$ (Rysgaard et al., 2013).

3.2 Observations at POLYI

Freeboard at POLYI was found to be negative and a slush layer was observed at the snow/ice interface. The snow base was generally characterized by a higher level of moisture relative to the ICEI and DNB sites. Observed CO_2 fluxes, meteorological parameters and components of the energy balance from the site are shown in Fig. 3. The prevailing wind direction (Fig. 3A) during the entire experiment was from the ice covered inner fjord (West) and the period was dominated by low to moderate wind speeds within the range $\mathrm{U} = 1 - 6\ \mathrm{ms^{-1}}$. Air temperature was recorded within the range $\mathrm{T_{air}} = -17 \pm 8°\mathrm{C}$ and followed a diurnal pattern with daily temperature changes on the order of $10°\mathrm{C}$ as well as a general incline of 5℃ during the experiment (Fig. 3A). We note that due to the relatively thin snow cover and cold atmosphere, the ice at this site was actively growing, as opposed to the thicker inner-fjord sites ICEI and DNB. CO_2 fluxes observed at POLYI (Fig. 3A) were both larger and more variable relative to observations at ICEI; $\mathrm{F_{CO2}} = -9.97 \pm 19.8\,\mathrm{mmol\,m^{-2}d^{-1}}$, where values given are the mean and standard deviation. Two chamber observations (Fig 3A, magenta diamonds), performed on the ice and in the snow on the 25th of March (Fig. 3A), both showed flux estimates on the order of concurrent eddy covariance flux estimates ($|\mathrm{F_{CO2}}| \leq 3.5\,\mathrm{mmol\,m^{-2}d^{-1}}$). Average net solar radiation during the experiment was slightly stronger than at ICEI; $\overline{\mathrm{R}}_\mathrm{n}^\mathrm{SW} = -40\ \mathrm{Wm^{-2}}$ (Fig. 3B). Sensible heat fluxes were observed within the range $\mathrm{Q_{SENS}} = \pm 20\,\mathrm{Wm^{-2}}$ with three events of strong heating and cooling recorded on the evening/night of the 24th of March, the midday/evening on the 25th of March and the early morning on the 27th of March (Fig. 3C). The only non-negligible latent heat fluxes were recorded on the morning of the 27th of March within the range $\mathrm{Q_{LAT}} = 1 \pm 1\,\mathrm{Wm^{-2}}$ (Fig. 3C). An ice-core observation on the 20th of March, five days before the initiation of eddy covariance measurements at POLYI, indicated a snow/ice interface temperature around $-5\,℃$ and calculated brine volume at around 12% (Rysgaard et al., 2013).

3.3 Observations at DNB

Freeboard at DNB was found to be negative and a thin slush layer was observed at the snow/ice interface in the beginning of the measurement period. Observed CO_2 fluxes, meteorological parameters and components of the energy balance from the site are shown in Fig. 4. The prevailing wind direction (Fig. 4A) during the entire experiment was from the ice-covered inner fjord (North-West) and the period was dominated by low wind speeds of $1 - 4\ \mathrm{ms^{-1}}$ with three events of very strong wind-speed of $6 - 10\ \mathrm{ms^{-1}}$ recorded on the 29th of March, the 9th-10th of April and on the 25th-26th of April respectively (Fig. 4A). Air temperature was recorded within the range of -19 ± 6 (Fig. 4A). The range of CO_2 fluxes observed at DNB (Fig. 4A) was the largest during the entire field-campaign; $\mathrm{F_{CO2}} = 8.64 \pm 39.64\,\mathrm{mmol\,m^{-2}d^{-1}}$, where values given are the mean and standard deviation. Average net solar radiation during the experiment was significantly higher than for both ICEI and POLYI; $\overline{\mathrm{R}}_\mathrm{n}^\mathrm{SW} = -75\mathrm{Wm^{-2}}$ (Fig. 4B). Sensible heat fluxes were predominantly within the range $\mathrm{Q_{SENS}} = \pm 50\ \mathrm{Wm^{-2}}$

with three events of strong surface heating ($Q_{SENS} = -100\ Wm^{-2}$) recorded on the 2nd, the 4th and the 7th of April, respectively (Fig. 4C). Latent heat fluxes were recorded within the range $Q_{LAT} = 3 \pm 3\ Wm^{-2}$ (Fig. 4C). Temperature readings of ice-cores (Attard, K., unpublished) taken a couple of days before the initiation of observations at the DNB site on the 26th and 28th of March respectively, indicated an increase in temperature from -4.7℃ to -4.0℃ at the snow/ice interface.

4 Data analysis and discussion

4.1 On the size of the CO_2-fluxes

The CO_2-fluxes observed during this experiment, particularly at POLYI and DNB, are comparable to the larger flux-rates reported in past studies over sea ice; $F_{CO2}^{ICE1} = 1.73 \pm 5\ \mathrm{mmol\ m^{-2}d^{-1}}$, $F_{CO2}^{POLY1} = -9.97 \pm 19.8\ \mathrm{mmol\ m^{-2}d^{-1}}$ and $F_{CO2}^{DNB} = 8.64 \pm 39.64\ \mathrm{mmol\ m^{-2}d^{-1}}$. Using eddy covariance instrumentation, CO_2-fluxes within the range $\pm 60\ \mathrm{mmol\ m^{-2}d^{-1}}$ have been measured over fast sea-ice near barrow, Alaska in June, 2002 (Semiletov et al., 2004). CO_2-fluxes within the range $-11 \pm 18\ \mathrm{mmol\ m^{-2}d^{-1}}$ have been observed in summer sea-ice from the western Weddell Sea, Antarctica (Zemmelink et al. 2006). CO_2-fluxes within the range $0.3 \pm 1.5\ \mathrm{mmol\ m^{-2}d^{-1}}$ were observed from a drifting ice-station in the Laptev sea during September, 2007 (Semiletov et al. 2007). Average CO_2-fluxes of $19.9\ \mathrm{mmol\ m^{-2}d^{-1}}$ and $32 \pm 5.2\ \mathrm{mmol\ m^{-2}d^{-1}}$ were observed on newly forming fast ice (30-40 cm thick) and on older fast ice respectively, in the Canadian arctic during November, 2007 through January, 2008 (Else et al., 2011). The authors also report strong uptake in areas of unconsolidated ice, open water and active leads. Daily average CO_2-fluxes within the range $7 \pm 67\ \mathrm{mmol\ m^{-2}d^{-1}}$ were reported on growing fast ice (0.8-1.7m thickness) in the Canadian arctic during January through June, 2004 (Miller et al., 2011b). CO_2-fluxes within the range $-78 \pm 180\ \mathrm{mmol\ m^{-2}d^{-1}}$ were reported on first-year ice in the Canadian arctic during May through June, 2002 (Papakyriakou and Miller, 2011). Using chamber instrumentation, CO_2-fluxes within the range $1.5 \pm 1.5\ \mathrm{mmol\ m^{-2}d^{-1}}$ were observed at ice-stations of various characteristics in the Canadian arctic during April through June, 2008 (Geilfus et al., 2012). The disparity in strength and direction of observed CO_2-fluxes at sites of different characteristics and at different time of year confirm that sea-ice is a very dynamic system and that further studies are necessary to understand the full potential of sea-ice in offsetting both regional- and global-scale carbon cycles. It is also possible that some of the fluxes derived using eddy covariance in the studies cited above contained a heating bias associated with the use of an older version of the open-path sensor (cf. Papakyriakou and Miller, 2011) In addition, a significant degree of disparity may be introduced by methodological challenges associated with eddy correlation observations in environments characterized by low fluxes and/or challenging topographical forcing of the ambient air flow (Sievers et al., 2015).

The fact that CO_2-fluxes at ICEI were close to zero may be because (1) calculated brine volume (Rysgaard et al., 2013) was just at the critical threshold for gas-permeability $V_B = 5.1\%$ (Golden et al., 1998; Loose et al., 2011a; Loose et al., 2011b), raising the possibility that brine transport was inhibited within the ice during that part of the experiment, and (2) the thick overlying snow cover prevented the free exchange of CO_2 in absence of wind-induced ventilation. We discuss the latter issue below. On the other hand, the stronger fluxes observed at POLYI may be attributed to thinner snow cover and brine transport in response to the much larger calculated brine volumes $V_B = 12\%$. Vertical brine transport and possible mixing with under-ice sea ice water (Zhou et al., 2013; Vancoppenolle et al., 2010) provides a mechanism for the brine wetting of the snow/ice interface and possibly of the snow-base. In this situation brine is close to the snow/atmosphere interface, not only allowing for an enhanced CO_2 exchange (particularly in the presence of a thinner snow cover) with the atmosphere, but also subject to more pronounced temperature shifts in response to the 24 h cycle of the diurnal energy budget at the site. As mentioned, changes in brine solubility of CO_2 and the dissolution/precipitation of $CaCO_3 \cdot 6H_2O$ associated with changing temperature provides for a dynamic air-ice pCO_2 gradient. Brine salinity and density increases with decreasing temperature (Petrich and Eiken, 2009). Hence, a temperature change may lead to convective mixing within the sea ice and underlying seawater, thereby coupling atmospheric exchange to conditions within the ice and ocean. Information on sea ice salinity, temperature, and therefore brine volume, were not available for the DNB site. The observation of larger CO_2-fluxes at this site is consistent with the notion that the brine volume at the snow/ice interface was well above the threshold for vertical mixing, and therefore for CO_2 exchange with the atmosphere. The snow/ice interface was warmer during the DNB time series relative to the ICEI and POLYI stages of the experiment (section 3.1-3.3), and therefore it is reasonable to assume that brine was present at the snow base and that processes affecting CO_2 speciation in the brine described above for POLYI remained active throughout the study period.

4.2 Processes controlling the CO_2 fluxes

4.2.1 Site energy fluxes

In order to investigate the association of the surface energy balance with CO_2 exchanges, we performed a diurnal correlation analysis (Fig. 5). Generally speaking, the limited observation time at both ICEI (Fig. 5A-E) and POLYI (Fig. 5F-J) leads to less certain definitions of diurnal patterns relative to that of the much longer time series obtained at DNB (Fig. 5K-O). The absence of turbulent observations during morning and noon, due to battery failures at the ICEI site is particularly clear in this illustration (Fig. 5A-E). Nevertheless, some patterns can be observed. At ICEI (Fig. 5A-E) outgassing of CO_2 coincides with radiative longwave cooling during nighttime (Fig. 5D) while uptake of CO_2 coincides with radiative shortwave warming during daytime (Fig. 5C). The net result is a positive correlation between net radiation and CO_2 fluxes ($R^2 = 0.34$) as seen in Fig. 5E. The same relations are evident at the similar, though warmer, DNB site (Fig. 5K-O). Outgassing of CO_2 coincides with nighttime radiative longwave cooling (Fig. 5N) while uptake or negligible CO_2 fluxes coincide with daytime radiative shortwave warming (Fig. 5M). Again, the net result is a positive correlation between net radiation and CO_2 fluxes ($R^2 = 0.47$) as seen in Fig. 5O. Unlike at ICEI, the clearly defined diurnal patterns at DNB also reveals a remarkable anti-correlation ($R^2 = 0.67$) between CO_2 fluxes and sensible heat fluxes (Fig. 5K). An association also observed over Antarctic sea ice by Zemmelink et al. (2006). Typically some positive correlation between turbulent parameters is expected considering their shared dependency on atmospheric flow conditions. An anti-correlation, however, is further indication of a connection between surface cooling (warming) and CO_2 outgassing (uptake).

It appears that much of the variability in CO_2 fluxes at ICEI and DNB can be explained by changes in the surface radiative balance. The plausible underlying thermochemical processes were discussed in section 4.2.1. At sea ice sites characterized by a thick ice cover, warming of the snow-ice interface, by way of radiative or oceanic influences, likely leads to brine dilution, brine volume expansion and $CaCO_3$ dissolution and hence a decrease in brine pCO_2 which ultimately drives enhanced uptake of CO_2 from the atmosphere. In contrast, cooling of the snow-ice interface likely leads to brine concentration, brine volume decrease and $CaCO_3$ formation and hence an increase in brine pCO_2 which ultimately drives enhanced outgassing of CO_2 into the atmosphere.

Equivalent relationships are less apparent at POLYI (Fig. 5F-J). There are indications of CO_2 uptake coinciding with radiative shortwave warming (Fig. 5H) and some CO_2 outgassing coinciding with radiative longwave cooling in the morning (Fig. 5I) but the pattern is broken by a consistent uptake of CO_2 coinciding with net radiative cooling in the late evening and night (Fig. 5J). It is important to note that the time series obtained at POLYI is very limited and so any conclusion drawn from these data might simply stem from the lack of a fully representative diurnal cycle. Nevertheless, a number of interpretations are possible: (1) surface cooling leads to convective mixing within the sea ice brines. Providing sufficiently permeable sea ice at the snow-ice interface, this couples atmospheric exchanges directly to overturning of high pCO_2 brines with comparatively low pCO_2 ocean water, thus facilitating an uptake of CO_2. This is supported here because all uptake of CO_2 in the period 2PM-1AM coincided with decreasing air temperatures (Fig. 3A). Note that some temporal lag between surface temperature changes and temperature changes within the ice should be expected. (2) As noted in the field, the site was characterized by high levels of moisture above the snow-ice interface. Such conditions might lead to the formation of superimposed ice within the snow, which has been found to inhibit gas exchanges (Nomura et al., 2010). This might explain the limited gas exchanges observed during the coldest part of the day (2AM-6AM). By extension we might expect a build-up of high pCO_2 brine during night at the snow-ice interface, which would explain the sudden burst of outward exchanges at 8AM when, presumably, warming of the superimposed ice and the snow-ice interface allows for the resumption of surface exchanges.

The fact that clear diurnal patterns of CO_2-fluxes can be described emphasizes that carbon budget estimates over sea ice should be based on sufficiently frequent sampling and not be restricted to snapshot measurements during the day.

4.2.2 Wind-speed

Given the indication of a relationship between CO_2-fluxes and the site energy balance, an appropriate evaluation of wind pumping requires the separation of thermochemical influences from any wind pumping effects. Furthermore, proper evaluation of wind pumping would have to account for the fact that correlation between wind speed and turbulent components, such as CO_2 fluxes, are expected under any circumstances. In the previous section we found that the best predictor for CO_2 fluxes was sensible heat fluxes (Fig. 5K). Here this correlation is re-evaluated in the context of wind-speed (Fig. 6). Two distinct mechanisms appear to be present, evident as a plausible thermochemical relationship between sensible heat fluxes and CO_2-fluxes ($R^2 = 0.41,\ P < 0.05$) during wind speeds within the range $0 - 9.5\ \mathrm{ms}^{-1}$ and a decoupled, less significant relationship ($R^2 = 0.26,\ P > 0.05$), during wind speeds within the range $9.5 - 11\ \mathrm{ms}^{-1}$. As expected, a positive relationship between turbulent components and wind speed is clearly evident for the proposed thermochemical relationship within the wind speed range $0 - 9.5\ \mathrm{ms}^{-1}$, while the same does not hold true for the relationship within the range $9.5 - 11\ \mathrm{ms}^{-1}$. The implication is that wind-pumping is a plausible additional process at the DNB site. No similar decoupling relationships were found at ICEI and POLYI. This may be due to the moderate wind speeds and the limited observation times. In addition, the moderate flux activity at ICEI could have also contributed to the lack of a decupled relationship, in that less CO_2 would have been stored in the snow under these circumstances. By extension, the presence of a thick snow cover might constitute a greater potential for snow pumping of stored CO_2. As such, this could explain the lack of a decoupled relationship at POLYI where snow thickness was moderate compared to the DNB site.

5 Conclusion

Eddy covariance observations of CO_2-fluxes were conducted during late winter at three locations on fast ice and newly formed polynya ice in a coastal fjord environment in North East Greenland. For the first time, CO_2-flux estimates over sea ice were derived using the Ogive optimization method (Sievers et al., 2015) shown to be an appropriate technique for quantifying small fluxes. Observations at the three sites were indicative of an environment experiencing the slow onset and gradual intensification of spring warming with average net solar radiation increasing from $-27\mathrm{Wm}^{-2}$ at ICEI to $-40\mathrm{Wm}^{-2}$ at POLYI and $-75\mathrm{Wm}^{-2}$ at DNB. Concurrent CO_2-flux estimates increased throughout the period: ICEI was characterized by negligible net CO_2 fluxes: $\mathrm{F}_{CO2} = 1.73 \pm 5\ \mathrm{mmol\,m^{-2}d^{-1}}$, POLYI was characterized by net CO_2 uptake $\mathrm{F}_{CO2} = -9.97 \pm 19.8\ \mathrm{mmol\,m^{-2}d^{-1}}$ and DNB was characterized by net CO_2 outgassing $\mathrm{F}_{CO2} = 8.64 \pm 39.64\ \mathrm{mmol\,m^{-2}d^{-1}}$. A diurnal correlation analysis supports a significant connection between site energetics and CO_2-fluxes linked to a number of possible thermally driven processes, which change the pCO_2 gradient at the snow-ice interface. The relative influence of these processes on atmospheric exchanges likely depends on the thickness of the ice. Specifically, the study indicates a predominant influence of brine volume expansion/contraction, brine dissolution/concentration and calcium carbonate formation/dissolution at sites characterized by a thick sea ice cover, such that surface warming leads to an uptake of CO_2 and vice versa, while convective overturning within the sea ice brines dominate at sites characterized by comparatively thin sea ice cover, such that nighttime surface cooling leads to an uptake of CO_2 to the extent permitted by simultaneous formation of superimposed ice in the lower snow-column. The existence of clear diurnal patterns of both energy fluxes and CO_2 fluxes emphasizes the importance of continuous and frequent sampling in order to properly resolve the respective budgets in a sea ice environment. In addition, a clear decoupling between CO_2 fluxes and the proposed thermochemical processes was observed at the DNB site at wind speeds exceeding the threshold $9.5 \mathrm{ms}^{-1}$, making wind-pumping a plausible second mechanism here. No similar relationships were found at the ICEI and POLYI sites, likely due to a combination of moderate wind speeds, limited observation time, limited flux activity (ICEI) and less thick snow cover (POLYI).

Acknowledgements

The study received financial support from the Arctic Research Centre, Aarhus University, the DEFROST project of the Nordic Centre of Excellence program “Interaction between Climate Change and the Cryosphere”, the collaborative research project “Changing Permafrost in the Arctic and its Global Effects in the 21st century” (PAGE21), the Canada Excellence Research Chair program, the Natural Sciences and Engineering Research Council of Canada (NSERC) and the ArcticNet Canadian network of centres of excellence. Additionally, this work is a contribution to the Arctic Science Partnership (ASP). We wish to thank the Greenland Survey (ASIAQ) for the use of radiation observations from the Zackenberg Research station. Søgaard, D.H. was supported financially by the Commission for Scientific Research in Greenland (KVUG). The authors furthermore wish to thank a number of people who assisted with the Daneborg experiment; Bruce Johnson, Kunuk Lennert, Ivali Lennert, Egon Randa Frandsen, Jens Ehn and Karl Attard.

References

Albert, M. R., Grannas, A. M., Bottenheim, J., Shepson, P. B., and Perron, F. E.: Processes and properties of snow-air transfer in the high Arctic with application to interstitial ozone at Alert, Canada, Atmos Environ, 36, 2779-2787, Pii S1352-2310(02)00118-8, Doi 10.1016/S1352-2310(02)00118-8, 2002.

Albert, M. R., and Shultz, E. F.: Snow and firn properties and air-snow transport processes at Summit, Greenland, Atmos Environ, 36, 2789-2797, Pii S1352-2310(02)00119-X, Doi 10.1016/S1352-2310(02)00119-X, 2002.

Anderson, L. G., Falck, E., Jones, E. P., Jutterström, S., and Swift, J. H.: Enhanced uptake of atmospheric CO2 during freezing of seawater: A field study in Storfjorden, Svalbard, Journal of Geophysical Research: Oceans, 109, C06004, 10.1029/2003JC002120, 2004.

Baldocchi, D.: Breathing of the terrestrial biosphere: lessons learned from a global network of carbon dioxide flux measurement systems, Aust J Bot, 56, 1-26, Doi 10.1071/Bt07151, 2008.

Barber, D. G., Papakyriakou, T. N., Ledrew, E. F., and Shokr, M. E.: An Examination of the Relation between the Spring Period Evolution of the Scattering Coefficient (Sigma-Degrees) and Radiative Fluxes over Landfast Sea-Ice, Int J Remote Sens, 16, 3343-3363, 1995a.

Barber, D. G., Reddan, S. P., and Ledrew, E. F.: Statistical Characterization of the Geophysical and Electrical-Properties of Snow on Landfast First-Year Sea-Ice, J Geophys Res-Oceans, 100, 2673-2686, Doi 10.1029/94jc02200, 1995b.

Barber, D. G., Ehn, J. K., Pućko, M., Rysgaard, S., Deming, J. W., Bowman, J. S., Papakyriakou, T., Galley, R. J., and Søgaard, D. H.: Frost flowers on young Arctic sea ice: The climatic, chemical and microbial significance of an emerging ice type, Journal of Geophysical Research: Atmospheres, 2014JD021736, 10.1002/2014JD021736, 2014.

Crocker, G. B.: A Physical Model for Predicting the Thermal-Conductivity of Brine-Wetted Snow, Cold Reg Sci Technol, 10, 69-74, Doi 10.1016/0165-232x(84)90034-X, 1984.

Delille, B., Jourdain, B., Borges, A. V., Tison, J. L., and Delille, D.: Biogas (CO2, O-2, dimethylsulfide) dynamics in spring Antarctic fast ice, Limnol Oceanogr, 52, 1367-1379, DOI 10.4319/lo.2007.52.4.1367, 2007.

Desjardins, R. L., Macpherson, J. I., Schuepp, P. H., and Karanja, F.: An Evaluation of Aircraft Flux Measurements of Co2, Water-Vapor and Sensible Heat, Bound-Lay Meteorol, 47, 55-69, Doi 10.1007/Bf00122322, 1989.

Dieckmann, G. S., Nehrke, G., Papadimitriou, S., Gottlicher, J., Steininger, R., Kennedy, H., Wolf-Gladrow, D., and Thomas, D. N.: Calcium carbonate as ikaite crystals in Antarctic sea ice, Geophys Res Lett, 35, Artn L08501, Doi 10.1029/2008gl033540, 2008.

Else, B. G. T., Papakyriakou, T. N., Galley, R. J., Drennan, W. M., Miller, L. A., and Thomas, H.: Wintertime CO2 fluxes in an Arctic polynya using eddy covariance: Evidence for enhanced air-sea gas transfer during ice formation, J Geophys Res-Oceans, 116, Artn C00g03, Doi 10.1029/2010jc006760, 2011.

Else, B. G. T., Papakyriakou, T. N., Raddatz, R., Galley, R. J., Mundy, C. J., Barber, D. G., Swystun, K., and Rysgaard, S.: Surface energy budget of landfast sea ice during the transitions from winter to snowmelt and melt pond onset: The importance of net longwave radiation and cyclone forcings, Journal of Geophysical Research: Oceans, 119, 3679-3693, 10.1002/2013JC009672, 2014.

Fischer, M., Thomas, D. N., Krell, A., Nehrke, G., Gottlicher, J., Norman, L., Meiners, K. M., Riaux-Gobin, C., and Dieckmann, G. S.: Quantification of ikaite in Antarctic sea ice, Antarct Sci, 25, 421-432, Doi 10.1017/S0954102012001150, 2013.

Foken, T., Wimmer, F., Mauder, M., Thomas, C., and Liebethal, C.: Some aspects of the energy balance closure problem, Atmos Chem Phys, 6, 4395-4402, 2006.

Ganot, Y., Dragila, M. I., and Weisbrod, N.: Impact of thermal convection on CO2 flux across the earth-atmosphere boundary in high-permeability soils, Agr Forest Meteorol, 184, 12-24, DOI 10.1016/j.agrformet.2013.09.001, 2014.

Geilfus, N. X., Carnat, G., Papakyriakou, T., Tison, J. L., Else, B., Thomas, H., Shadwick, E., and Delille, B.: Dynamics of pCO(2) and related air-ice CO2 fluxes in the Arctic coastal zone (Amundsen Gulf, Beaufort Sea), J Geophys Res-Oceans, 117, Artn C00g10, Doi 10.1029/2011jc007118, 2012.

Geilfus, N. X., Carnat, G., Dieckmann, G. S., Halden, N., Nehrke, G., Papakyriakou, T., Tison, J. L., and Delille, B.: First estimates of the contribution of CaCO3 precipitation to the release of CO2 to the atmosphere during young sea ice growth, Journal of Geophysical Research: Oceans, 118, 244-255, 10.1029/2012JC007980, 2013.

Golden, K. M., Ackley, S. F., and Lytle, V. I.: The percolation phase transition in sea ice, Science, 282, 2238-2241, DOI 10.1126/science.282.5397.2238, 1998.

Jones, H. G., Pomeroy, J. W., Davies, T. D., Tranter, M., and Marsh, P.: CO2 in Arctic snow cover: landscape form, in-pack gas concentration gradients, and the implications for the estimation of gaseous fluxes, Hydrol Process, 13, 2977-2989, 1999.

Killawee, J. A., Fairchild, I. J., Tison, J. L., Janssens, L., and Lorrain, R.: Segregation of solutes and gases in experimental freezing of dilute solutions: Implications for natural glacial systems, Geochim Cosmochim Ac, 62, 3637-3655, Doi 10.1016/S0016-7037(98)00268-3, 1998.

Lizotte, M. P.: The contributions of sea ice algae to Antarctic marine primary production, Am Zool, 41, 57-73, Doi 10.1668/0003-1569(2001)041[0057:Tcosia]2.0.Co;2, 2001.

Loose, B., Miller, L. A., Elliott, S., and Papakyriakou, T.: Sea Ice Biogeochemistry and Material Transport Across the Frozen Interface, Oceanography, 24, 202-218, 2011a.

Loose, B., Schlosser, P., Perovich, D., Ringelberg, D., Ho, D. T., Takahashi, T., Richter-Menge, J., Reynolds, C. M., McGillis, W. R., and Tison, J. L.: Gas diffusion through columnar laboratory sea ice: implications for mixed-layer ventilation of CO2 in the seasonal ice zone, Tellus B, 63, 23-39, DOI 10.1111/j.1600-0889.2010.00506.x, 2011b.

Marion, G. M.: Carbonate mineral solubility at low temperatures in the Na-K-Mg-Ca-H-Cl-SO4-OH-HCO3-CO3-CO2-H2O system, Geochim Cosmochim Ac, 65, 1883-1896, Doi 10.1016/S0016-7037(00)00588-3, 2001.

Massman, W. J., and Frank, J. M.: Advective transport of CO2 in permeable media induced by atmospheric pressure fluctuations: 2. Observational evidence under snowpacks, J Geophys Res-Biogeo, 111, Artn G03005, Doi 10.1029/2006jg000164, 2006.

Miller, L. A., Carnat, G., Else, B. G. T., Sutherland, N., and Papakyriakou, T. N.: Carbonate system evolution at the Arctic Ocean surface during autumn freeze-up, J Geophys Res-Oceans, 116, Artn C00g04, Doi 10.1029/2011jc007143, 2011a.

Miller, L. A., Papakyriakou, T. N., Collins, R. E., Deming, J. W., Ehn, J. K., Macdonald, R. W., Mucci, A., Owens, O., Raudsepp, M., and Sutherland, N.: Carbon dynamics in sea ice: A winter flux time series, J Geophys Res-Oceans, 116, Artn C02028, Doi 10.1029/2009jc006058, 2011b.

Nomura, D., Yoshikawa-Inoue, H., and Toyota, T.: The effect of sea-ice growth on air-sea CO2 flux in a tank experiment, Tellus B, 58, 418-426, DOI 10.1111/j.1600-0889.2006.00204.x, 2006.

Nomura, D., Yoshikawa-Inoue, H., Toyota, T., and Shirasawa, K.: Effects of snow, snowmelting and refreezing processes on air-sea-ice CO2 flux, J Glaciol, 56, 262-270, 2010.

Nomura, D., Assmy, P., Nehrke, G., Granskog, M. A., Fischer, M., Dieckmann, G. S., Fransson, A., Hu, Y. B., and Schnetger, B.: Characterization of ikaite (CaCO3 center dot 6H(2)O) crystals in first-year Arctic sea ice north of Svalbard, Ann Glaciol, 54, 125-131, Doi 10.3189/2013aog62a034, 2013.

Papadimitriou, S., Kennedy, H., Kattner, G., Dieckmann, G. S., and Thomas, D. N.: Experimental evidence for carbonate precipitation and CO2 degassing during sea ice formation, Geochim Cosmochim Ac, 68, 1749-1761, DOI 10.1016/j.gca.2003.07.004, 2004.

Papakyriakou, T., and Miller, L.: Springtime CO2 exchange over seasonal sea ice in the Canadian Arctic Archipelago, Ann Glaciol, 52, 215-224, 2011.
Parmentier, F. J. W., Christensen, T. R., Sorensen, L. L., Rysgaard, S., McGuire, A. D., Miller, P. A., and Walker, D. A.: The impact of lower sea-ice extent on Arctic greenhouse-gas exchange, Nat Clim Change, 3, 195-202, Doi 10.1038/Nclimate1784, 2013.
Perovich, D. K., and Richtermenge, J. A.: Surface Characteristics of Lead Ice, J Geophys Res-Oceans, 99, 16341-16350, Doi 10.1029/94jc01194, 1994.
Persson, P. O. G.: Onset and end of the summer melt season over sea ice: thermal structure and surface energy perspective from SHEBA, Clim Dynam, 39, 1349-1371, DOI 10.1007/s00382-011-1196-9, 2012.
Petrich, C., and Eiken, H.: Growth, structure and properties of sea ice, in Thomas, D.N. and Dieckmann, G.S. (eds.) Sea Ice, pp. 23-77, Wiley-Blackwell, Oxford, UK., 2009.
Powers, D., Colbeck, S. C., and Oneill, K.: Experiments on Thermal-Convection in Snow, Ann Glaciol, 6, 43-47, 1985.
Rysgaard, S., Glud, R. N., Sejr, M. K., Bendtsen, J., and Christensen, P. B.: Inorganic carbon transport during sea ice growth and decay: A carbon pump in polar seas, J Geophys Res-Oceans, 112, Artn C03016, Doi 10.1029/2006jc003572, 2007.
Rysgaard, S., Bendtsen, J., Pedersen, L. T., Ramlov, H., and Glud, R. N.: Increased CO2 uptake due to sea ice growth and decay in the Nordic Seas, J Geophys Res-Oceans, 114, Artn C09011, Doi 10.1029/2008jc005088, 2009.
Rysgaard, S., Bendtsen, J., Delille, B., Dieckmann, G. S., Glud, R. N., Kennedy, H., Mortensen, J., Papadimitriou, S., Thomas, D. N., and Tison, J. L.: Sea ice contribution to the air-sea CO2 exchange in the Arctic and Southern Oceans, Tellus B, 63, 823-830, DOI 10.1111/j.1600-0889.2011.00571.x, 2011.
Rysgaard, S., Glud, R. N., Lennert, K., Cooper, M., Halden, N., Leakey, R. J. G., Hawthorne, F. C., and Barber, D.: Ikaite crystals in melting sea ice - implications for pCO(2) and pH levels in Arctic surface waters, Cryosphere, 6, 901-908, DOI 10.5194/tc-6-901-2012, 2012.
Rysgaard, S., Sogaard, D. H., Cooper, M., Pucko, M., Lennert, K., Papakyriakou, T. N., Wang, F., Geilfus, N. X., Glud, R. N., Ehn, J., McGinnis, D. F., Attard, K., Sievers, J., Deming, J. W., and Barber, D.: Ikaite crystal distribution in winter sea ice and implications for CO2 system dynamics, Cryosphere, 7, 707-718, DOI 10.5194/tc-7-707-2013, 2013.
Sahlee, E., Smedman, A. S., Rutgersson, A., and Hogstrom, U.: Spectra of CO2 and water vapour in the marine atmospheric surface layer, Bound-Lay Meteorol, 126, 279-295, DOI 10.1007/s10546-007-9230-5, 2008.
Semiletov, I., Makshtas, A., Akasofu, S. I., and Andreas, E. L.: Atmospheric CO(2) balance: The role of Arctic sea ice, Geophys Res Lett, 31, Artn L05121, Doi 10.1029/2003gl017996, 2004.
Semiletov, I. P., Pipko, I. I., Repina, I., and Shakhova, N. E.: Carbonate chemistry dynamics and carbon dioxide fluxes across the atmosphere-ice-water interfaces in the Arctic Ocean: Pacific sector of the Arctic, J Marine Syst, 66, 204-226, DOI 10.1016/j.jmarsys.2006.05.012, 2007.
Seok, B., Helmig, D., Williams, M. W., Liptzin, D., Chowanski, K., and Hueber, J.: An automated system for continuous measurements of trace gas fluxes through snow: an evaluation of the gas diffusion method at a subalpine forest site, Niwot Ridge, Colorado, Biogeochemistry, 95, 95-113, DOI 10.1007/s10533-009-9302-3, 2009.
Sievers, J., Papakyriakou, T., Larsen, S. E., Jammet, M. M., Rysgaard, S., Sejr, M. K., and Sørensen, L. L.: Estimating surface fluxes using eddy covariance and numerical ogive optimization, Atmos. Chem. Phys., 15, 2081-2103, 10.5194/acp-15-2081-2015, 2015.
Sogaard, D. H., Thomas, D. N., Rysgaard, S., Glud, R. N., Norman, L., Kaartokallio, H., Juul-Pedersen, T., and Geilfus, N. X.: The relative contributions of biological and abiotic processes to carbon dynamics in subarctic sea ice, Polar Biol, 36, 1761-1777, DOI 10.1007/s00300-013-1396-3, 2013.

Sørensen, L. L., Jensen, B., Glud, R. N., McGinnis, D. F., Sejr, M. K., Sievers, J., Søgaard, D. H., Tison, J. L., and Rysgaard, S.: Parameterization of atmosphere–surface exchange of CO2 over sea ice, The Cryosphere, 8, 853-866, 10.5194/tc-8-853-2014, 2014.

Sturm, M.: The role of thermal convection in heat and mass transport in the subarctic snow-cover, Cold Regions Research and Engineering Laboratory (U.S.), Army Corps of Engineers Cold Regions Research & Engineering Laboratory, CRREL Technical Report 91-19, 1991.

Sturm, M., Perovich, D. K., and Holmgren, J.: Thermal conductivity and heat transfer through the snow on the ice of the Beaufort Sea, J Geophys Res-Oceans, 107, Artn 8043, Doi 10.1029/2000jc000409, 2002.

Takagi, K., Nomura, M., Ashiya, D., Takahashi, H., Sasa, K., Fujinuma, Y., Shibata, H., Akibayashi, Y., and Koike, T.: Dynamic carbon dioxide exchange through snowpack by wind-driven mass transfer in a conifer-broadleaf mixed forest in northernmost Japan, Global Biogeochem Cy, 19, Artn Gb2012, Doi 10.1029/2004gb002272, 2005.

Thomas, D. N., and Dieckmann, G. S.: Sea Ice, 2 ed., Oxford, Wiley-Blackwell, 2010.

Tison, J. L., Haas, C., Gowing, M. M., Sleewaegen, S., and Bernard, A.: Tank study of physico-chemical controls on gas content and composition during growth of young sea ice, J Glaciol, 48, 177-191, Doi 10.3189/172756502781831377, 2002.

Vancoppenolle, M., Goosse, H., de Montety, A., Fichefet, T., Tremblay, B., and Tison, J. L.: Modeling brine and nutrient dynamics in Antarctic sea ice: The case of dissolved silica, J Geophys Res-Oceans, 115, Artn C02005, Doi 10.1029/2009jc005369, 2010.

Zemmelink, H. J., Delille, B., Tison, J. L., Hintsa, E. J., Houghton, L., and Dacey, J. W. H.: CO(2) deposition over the multi-year ice of the western Weddell Sea, Geophys Res Lett, 33, Artn L13606, Doi 10.1029/2006gl026320, 2006.

Zhou, J., Delille, B., Eicken, H., Vancoppenolle, M., Brabant, F., Carnat, G., Geilfus, N.-X., Papakyriakou, T., Heinesch, B., and Tison, J.-L.: Physical and biogeochemical properties in landfast sea ice (Barrow, Alaska): Insights on brine and gas dynamics across seasons, Journal of Geophysical Research: Oceans, 118, 3172-3189, 10.1002/jgrc.20232, 2013.

Figures

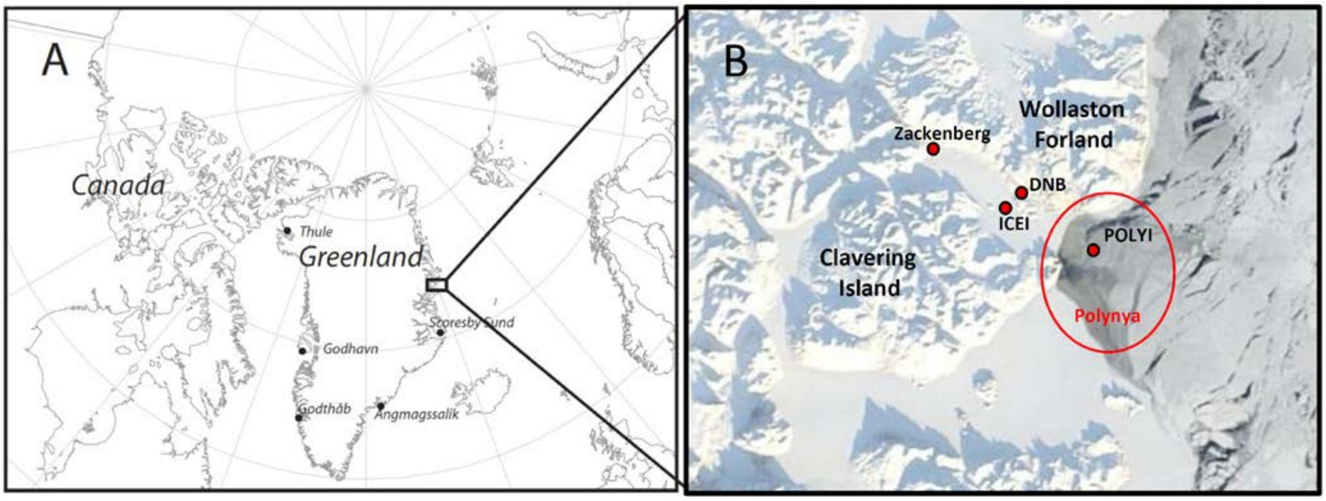

Figure 1: (A) Regional and **(B)** local overview of field-sites in Young-Sound, NE Greenland. Sites ICEI and DNB were located in the inner-fjord characterized by thick fast sea ice and a thick snow-cover, and POLYI was located in an active polynia, characterized by thin ice and snow-cover.

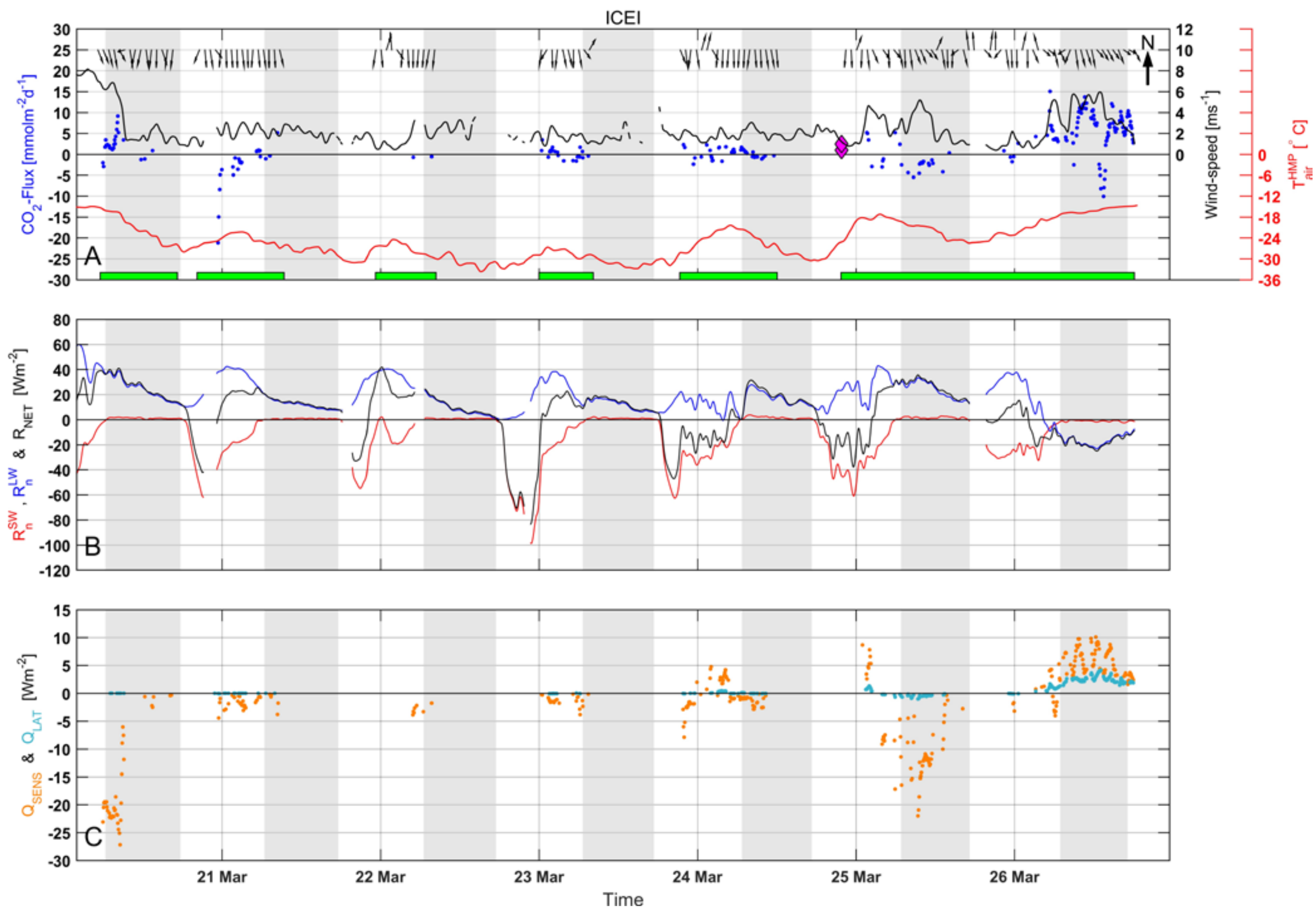

Figure 2: ICEI timeseries of **(A)** EC derived CO_2-fluxes (blue markers), chamber observations of CO_2-flux (magenta diamonds), wind-speed (black line), HMP air temperature (red line) and wind-direction (black arrows). Wind-direction due north is indicated in the upper right corner. Green bars indicate when the EC instruments were online; **(B)** net shortwave radiation (red line), net longwave radiation (blue line) and net radiation (black line); **(C)** turbulent sensible heat flux (orange dots) and turbulent latent heat flux (light-blue dots). Grey shaded areas indicate night-time.

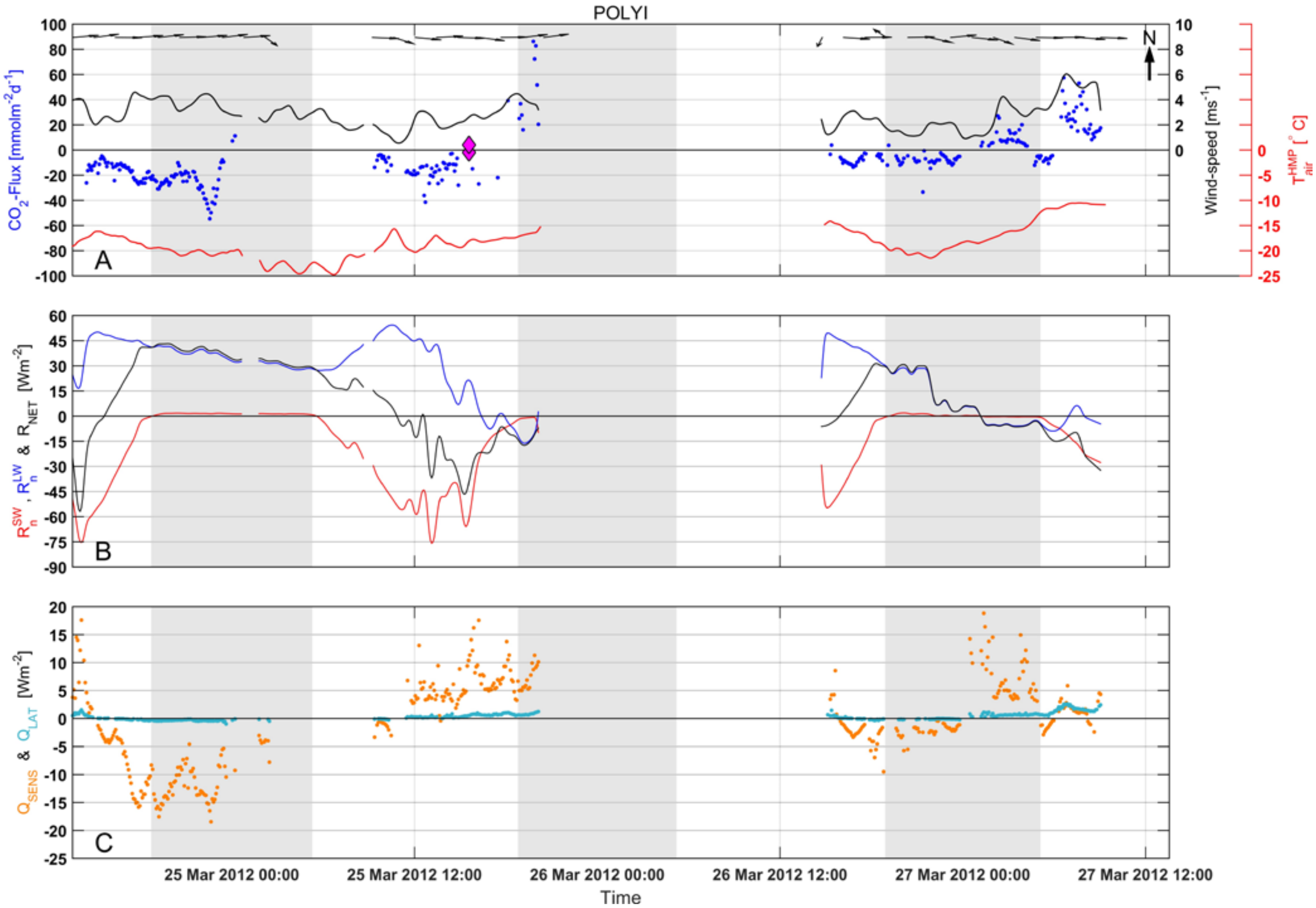

Figure 3: POLYI timeseries shown as for Fig. 2, but without green bars indicating instrument status in (A).

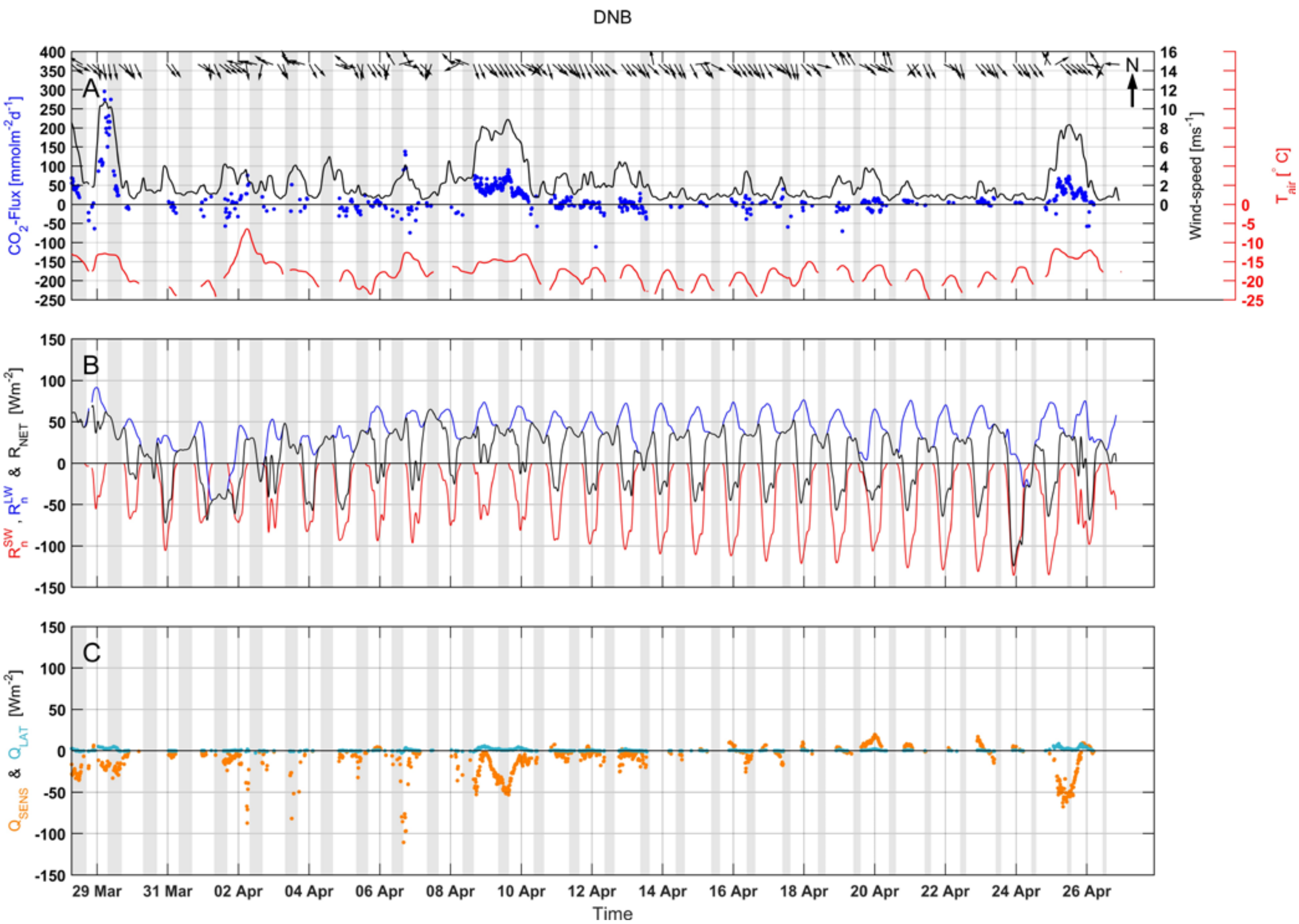

Figure 4: DNB timeseries shown as for Fig. 2, but without green bars indicating instrument status in (A).

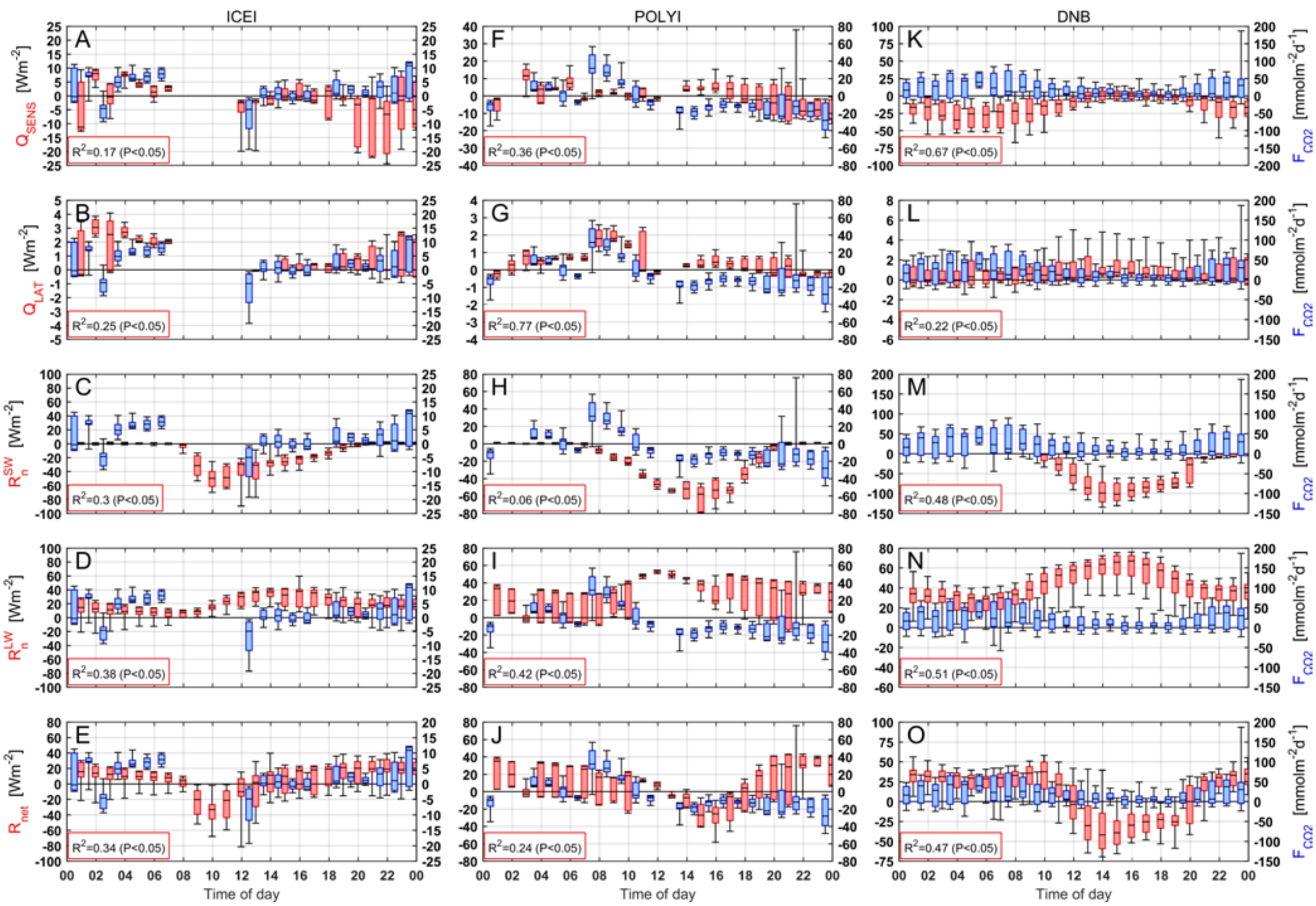

Figure 5: Diurnal patterns of **(AFK)** sensible heat flux **(BGL)** latent heat flux **(CHM)** net shortwave energy **(DIN)** net longwave energy and **(EJO)** net radiative energy (red boxplots) shown alongside the diurnal pattern of CO_2-fluxes (blue boxplots) for the three experimental sites in question (columns). Boxplots are composed of the median (black middle line), the 25-75th percentile (box) and the 9-91st percentile (black whiskers) respectively. Correlations are indicated along with P-values in red boxes in the lower-left corner of each graph. In order to account for outliers the correlations given are the best among four diurnal correlations based on either all data, the 9-91th percentile, the 25-75th percentile or the medians, for which $P < 0.05$.

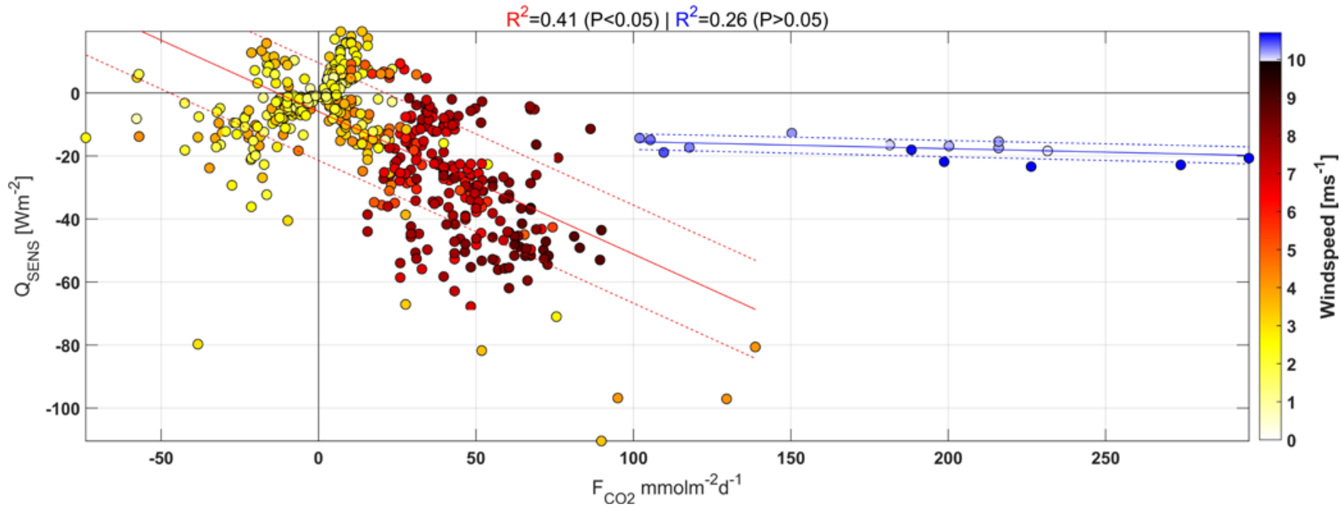

Figure 6: Correlations between sensible heat flux and CO_2 fluxes for the DNB site, colorcoded according to wind speed.